ChemCatChem

Research Article
doi.org/10.1002/cctc.202101756

Chemistry Europe
European Chemical Societies Publishing

www.chemcatchem.org

Aluminum-based Metal-Organic Framework as Water-tolerant Lewis Acid Catalyst for Selective Dihydroxyacetone Isomerization to Lactic Acid

Mohammad Shahinur Rahaman,*[a] Sarttrawut Tulaphol,[b] Kyle Mills,[a] Ashten Molley,[a] Md Anwar Hossain,[a] Shashi Lalvani,[c] Thana Maihom,[d] Mark Crocker,[e, f] and Noppadon Sathitsuksanoh*[a]

Lactic acid is a renewable and versatile chemical for food, pharmaceuticals, cosmetics, and other chemicals. Lactic acid can be produced from biomass-derived dihydroxyacetone. However, selective and recyclable water-tolerant acid catalysts need to be developed for the specific production of lactic acid. Here we show that the MIL-101(Al)–NH_2 metal-organic framework (MOF) is a water-tolerant and selective solid Lewis acid catalyst for dihydroxyacetone isomerization to lactic acid. The Lewis acidic MIL-101(Al)–NH_2 catalyst promoted a high lactic acid selectivity of 91% at 96% dihydroxyacetone conversion at 120 °C in water. The reaction proceeded by temperature and/or MIL-101(Al)–NH_2 MOFs mediated dihydroxyacetone dehydration to pyruvaldehyde. Subsequently, the MIL-101(Al)–NH_2 facilitated rehydration of the pyruvaldehyde to lactic acid. The Lewis acidic MIL-101(Al)–NH_2 catalyst was stable and reusable four times without any decrease in catalytic performance.

Introduction

Lactic acid is an important platform chemical for biodegradable polylactic acid, propylene glycol, and acrylic acid.[1] Lactic acid can be produced by acid-catalyzed isomerization of dihydroxyacetone, obtained from biomass-derived glycerol, xylose,[2–6] or fructose.[7] This acid-catalyzed isomerization reaction proceeds by a cascade of dihydroxyacetone dehydration to pyruvaldehyde and subsequent pyruvaldehyde rehydration to lactic acid (Scheme 1).[8–9] The challenge in lactic acid production is the development of effective and selective water-tolerant acid catalysts.[10]

Jolimaitre et al.[11] and Rasrendra et al.[9] showed that Al^{3+} Lewis acid salts were active and selective for dihydroxyacetone conversion to lactic acid. For example, Rasrendra et al. reported a high lactic acid yield of 90% at 100% dihydroxyacetone conversion by $AlCl_3$.[9] However, the reaction with Lewis acid salts presents a classic problem of catalyst separation and product purification that contributes to the production cost of lactic acid. Sun et al. used Sn-containing β-zeolites, unique solid Lewis acid catalysts, and achieved an attractive lactic acid yield

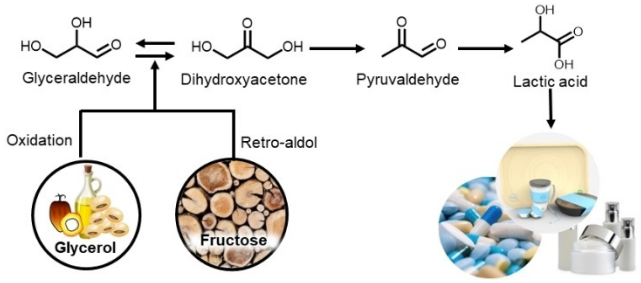

Scheme 1. Chemical pathway for lactic acid production and its use.

[a] M. S. Rahaman, K. Mills, A. Molley, M. A. Hossain, Prof. N. Sathitsuksanoh
Department of Chemical Engineering
University of Louisville
216 Eastern Pkwy
Louisville, KY 40208 (USA)
E-mail: shahinur.rahaman08@gmail.com
armlab15@gmail.com
n.sathitsuksanoh@louisville.edu
Homepage: http://tikgroup.org
[b] Dr. S. Tulaphol
Sustainable Polymer & Innovative Composite Materials Research Group
Department of Chemistry
Faculty of Science
King Mongkut's University of Technology Thonburi
126 Pracha Uthit Road
Bang Mot
Thung Khru, Bangkok 10140 (Thailand)
[c] Prof. S. Lalvani
Department of Chemical, Paper and Biomedical Engineering
Miami University
64 Engineering Building
650 E. High St.
Oxford,OH 45056 (USA)
[d] Dr. T. Maihom
Department of Chemistry
Faculty of Liberal Arts and Science
Kasetsart University
Kamphaeng Saen Campus
Nakhon Pathom 73140 (Thailand)
[e] Prof. M. Crocker
Center for Applied Energy Research,
University of Kentucky
2540 Research Park Drive
Lexington, KY 40511 (USA)
[f] Prof. M. Crocker
Department of Chemistry
University of Kentucky
161 Jacobs Science Building
Lexington, KY 40506 (USA)

Supporting information for this article is available on the WWW under https://doi.org/10.1002/cctc.202101756

of 86% from dihydroxyacetone.[12] The Lewis acid sites in Sn-β zeolites are hypothesized to be responsible for the high lactic acid selectivity. Although Sn-containing zeolites are active for dihydroxyacetone conversion, they deactivated after three cycles due to the formation of coke and humins that prevent diffusion of substrates.[13] Moreover, they could not be regenerated after calcining at 300–550 °C for 3–6 h. Alternatively, Dapsens et al. described the desilication of commercial ZSM-5 zeolites and achieved >90% lactic acid selectivity at 91% conversion at 140 °C for 6 h.[14] However, desilication weakens the zeolite's mechanical strength and severely damages the microporous framework.[15–16] Thus, the industry needs efficient heterogeneous catalysts with recyclability for dihydroxyacetone isomerization to lactic acid.

Inspired by the high activity and selectivity of Al Lewis acid salts for dihydroxyacetone isomerization to lactic acid,[9,11] we set out to develop an efficient Al-derived solid Lewis acid catalyst. To do so, we investigated the catalytic activity of Al-based metal-organic frameworks (MOFs). Metal-organic frameworks are porous crystalline materials composed of metal clusters (nodes) connected by organic ligands that form coordination networks.[17–19] Metal-organic frameworks are attractive materials because of the ability to tailor metal centers, pore size, and functional groups along with an ease in synthesis compared with zeolitic materials. As a result, metal-organic frameworks have been used in many applications, such as energy storage,[20–21] gas adsorption,[22] drug delivery,[23] and solid catalysts.[17–18] Importantly for our goal, the exposed metal nodes endow MOFs with Lewis acid sites, and the tunability of their linker can enhance MOF catalytic ability. These attributes make MOFs attractive as solid Lewis acid catalysts. Yet, although MOFs are promising catalysts for the chemical industry, they adsorb water quickly, which blocks the active sites and compromises MOF catalytic activity.[24–29]

In this work, we showed that the MIL-101(Al)–NH_2 (Al-MOF) was a water-tolerant and active solid Lewis acid catalyst for selective dihydroxyacetone isomerization to lactic acid. The Al-MOF gave a high lactic acid yield of 88% at 120 °C after 24 h. Furthermore, we reused Al-MOF four times without loss of catalytic performance.

Results

Physicochemical properties of the catalysts

To assess our catalyst's physical and chemical properties, we characterized MIL-101(Al)–NH_2 (Al-MOF) by XRD, N_2 adsorption-desorption, TGA, FTIR, ICP-OES, and HRTEM (Figure S1). The N_2 adsorption-desorption assay of the MIL-101(Al)–NH_2 showed a type IV isotherm, which suggested the mesoporous characteristic of Al-MOF.[30] The calculated surface area and pore volume were 1487 m^2/g and 0.92 cc/g (Table S2), respectively, similar to reported values.[30–35] As a control, the surface area and pore volume of γ-Al_2O_3 was 191 m^2/g and 0.5 cc/g, respectively, in agreement with a report by Samad et al.[36] The XRD pattern of MIL-101(Al)–NH_2 coincided with the simulated MIL-101 framework, which confirmed the formation of the MIL-101 structure.[30,35] The STEM-HAADF images and elemental phase mapping of aluminum of MIL-101(Al)–NH_2 showed that this material was porous, and aluminum was highly dispersed (Figure S1C–D). The inductively coupled plasma-optical emission spectroscopy (ICP-OES) showed that MIL-101(Al)–NH_2 had an aluminum content of 11.6 wt.%.

To confirm the presence of functional groups and the thermal stability of our MIL-101(Al)–NH_2, we performed FTIR and TGA (Figure S1E–G). The FTIR spectrum of MIL-101(Al)–NH_2 showed bands corresponding to the symmetric and asymmetric stretching of primary amines (3390 and 3500 cm^{-1}) (Figure S1F). The presence of these amine bands suggested that the amino groups (–NH_2 groups) were free without coordination. Furthermore, the shoulder at 1624 cm^{-1} corresponded to the N–H scissoring vibration. The band at 1336 cm^{-1} corresponded to the C–N stretching absorption of aromatic amines, which confirmed the presence of –NH_2 groups in the MOF.[33] Thermal stability is an essential property of catalysts to ensure continuous operation without losing their structural integrity and catalytic performance. The TGA profile of MIL-101(Al)–NH_2 exhibited three mass loss zones between 30–150 °C (~10 wt. %), 150–380 °C (~20 wt. %), and 380–680 °C (~33 wt. %). These mass reductions corresponded, respectively, to (1) the evaporation of the water molecules, (2) the degradation of organic linkers, and (3) the degradation of the organic 2-aminoterephthalic acid-Al^{3+} complexes.

Acid properties of the catalysts

Selective dihydroxyacetone isomerization to lactic acid requires acid catalysts for the cascade of dihydroxyacetone dehydration to pyruvaldehyde, followed by pyruvaldehyde rehydration to lactic acid. Hence, it is essential to distinguish and quantify the acid sites of catalysts. To characterize the acid sites, we performed temperature-programmed desorption using DRIFTS with adsorbed pyridine on γ-Al_2O_3 and MIL-101(Al)–NH_2 (Figure 1). Currently, there are no ideal techniques for acid site identification and determination for MOFs.[37] We chose pyridine as an in-situ titrant for probing the acid site density of MOFs because of previous observations of Lewis acid and Brønsted

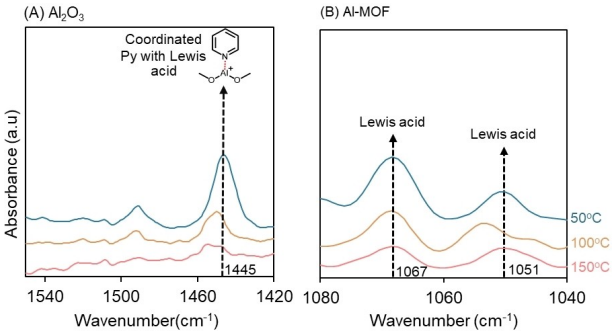

Figure 1. Diffuse reflectance infrared Fourier transform (DRIFT) spectra of adsorbed pyridine with γ-Al_2O_3 (A) and MIL-101(Al)–NH_2 (B).

acid sites in MOFs.[38–40] The DRIFT spectrum of MIL-101(Al)–NH_2 MOF had characteristic bands at 1067 and 1051 cm^{-1}, corresponding to the coordination between pyridine and Lewis acid sites from the Al^{3+} metal center.[41–42] The intensity of the bands for both catalysts decreased with increasing desorption temperature from 50 to 150 °C. The band for γ-Al_2O_3 at 1445 cm^{-1} almost disappeared at 150 °C. Conversely, the Al-MOF displayed a comparatively stronger band at 1067 and 1051 cm^{-1} at 150 °C, which suggested that it had stronger Lewis acid sites compared with the γ-Al_2O_3. The DRIFT spectra of adsorbed pyridine enabled determination of Lewis acid site density (Table S2). DRIFT results suggested that MIL-101(Al)–NH_2 had a greater Lewis acid strength and site density compared with γ-Al_2O_3.

Screening of aluminum-containing catalysts for dihydroxyacetone conversion

We measured the efficiency of the dihydroxyacetone isomerization to lactic acid by evaluating the catalytic performance of selected aluminum-containing catalysts in water at 90 °C for 4 h and a dihydroxyacetone:Al molar ratio of 14:1 (Figure 2). Pyruvaldehyde and lactic acid were the primary reaction products. Our blank (without catalyst) experiment showed < 5% dihydroxyacetone conversion. These results indicated that catalysts were needed to facilitate this reaction. The γ-Al_2O_3 was the most active with 42.7% dihydroxyacetone conversion. However, these catalysts differed in lactic acid productivity, with MIL-101(Al)–NH_2 having the greatest productivity of 0.62 h^{-1}. All Al-containing homogeneous catalysts showed higher productivity compared with γ-Al_2O_3 (Table S3). For comparison, we calculated the productivity on the basis of total gram of catalyst (*see Supporting Information for details*). We also compared the catalytic activity of dihydroxyacetone isomerization to lactic acid by MIL-101(Al)–NH_2 and $AlCl_3.6H_2O$ at 90 °C for 24 h (Figure S2). With the high catalytic activity, product selectivity, and potential reuse, we chose MIL-101(Al)–NH_2 for further studies as a water-tolerant solid Lewis acid catalyst.

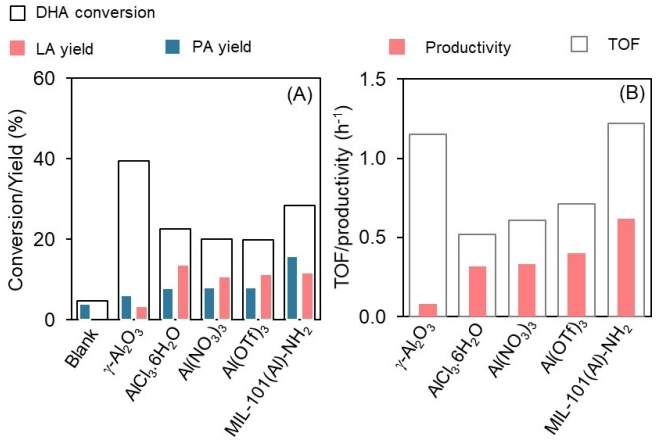

Figure 2. Catalytic activity of MIL-101(Al)–NH_2 and aluminum-containing homogenous and heterogeneous catalysts, conversion/yield (A), and TOF/productivity (B). Reaction condition. dihydroxyacetone: Al molar ratio = 14:1, 90 °C, 4 h, 10 mg dihydroxyacetone in 2 g water. DHA, PA, and LA indicates dihydroxyacetone, pyruvaldehyde, and lactic acid, respectively.

Effect of Lewis acid sites of MIL-101(Al)–NH_2 MOF on dihydroxyacetone conversion

Next, we examined the product evolution of MIL-101(Al)–NH_2 by comparing with blank (no catalyst) and γ-Al_2O_3 as our controls at 90 °C (Figure 3). We chose γ-Al_2O_3 as a proxy for solid Lewis acid catalyst.[43–45] The blank gave 9.6% pyruvaldehyde yield at 19.1% dihydroxyacetone conversion at 90 °C after 24 h. We did not observe any lactic acid. For γ-Al_2O_3, dihydroxyacetone conversion progressively increased and reached 90% after 24 h. However, we observed a low yield of lactic acid (16%) and pyruvaldehyde (< 10%) after 24 h. We observed a brown substance on the γ-Al_2O_3 surface and in the reaction mixture, which indicated formation of unwanted humin. Our observation of humin was in agreement with previous studies using zeolites[46] and Al_2O_3[47] as catalysts for dihydroxyacetone conversion. The Al-MOF demonstrated a progressive increase in lactic acid yield and reached 74% at 84% dihydroxyacetone conversion after 24 h. An increase in lactic acid yield and conversion of dihydroxyacetone with time suggested that Al-MOF was active and selective to lactic acid.

To elucidate the effect of the Lewis acid sites of MIL-101(Al)–NH_2 and γ-Al_2O_3 catalysts on the dihydroxyacetone dehydration and pyruvaldehyde rehydration, we plotted lactic acid and pyruvaldehyde selectivity versus dihydroxyacetone conversion (Figure 4). MIL-101(Al)–NH_2 showed high lactic acid selectivity (88%) compared with γ-Al_2O_3 at similar DHA conversion, which corroborated a greater Lewis acid strength and site density of MIL-101(Al)–NH_2 compared with γ-Al_2O_3 (Figure 1 & Table S2). Thus, the results suggested that Lewis acid sites were important in selective dihydroxyacetone isomerization to lactic acid.

We observed pyruvaldehyde as our reaction product in our blank experiment (Figure 3A). Hence, we could not rule out temperature-mediated dihydroxyacetone dehydration to pyru-

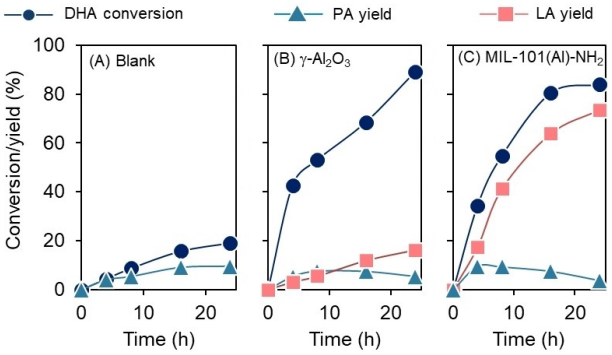

Figure 3. Catalytic activity of blank (A), γ-Al_2O_3 (B), and MIL-101(Al)–NH_2 (C). Reaction condition. dihydroxyacetone: Al molar ratio = 14:1, 90 °C, 10 mg dihydroxyacetone in 2 g water. DHA, PA, and LA indicates dihydroxyacetone, pyruvaldehyde, and lactic acid, respectively.

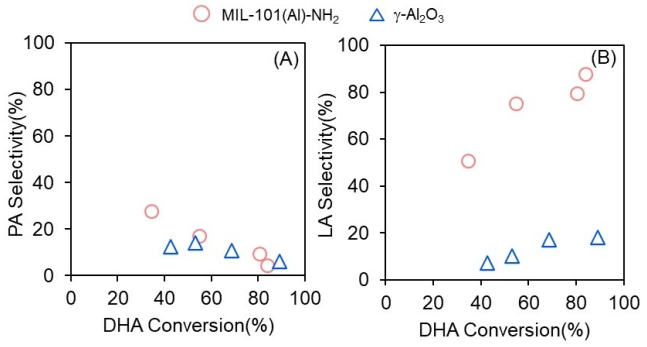

Figure 4. Comparison of catalytic activity of dihydroxyacetone isomerization to lactic acid at 90 °C by MIL-101(Al)–NH_2 and γ-Al_2O_3. Relationships between pyruvaldehyde selectivity vs dihydroxyacetone conversion (A) and lactic acid selectivity vs dihydroxyacetone conversion (B). Reaction condition. dihydroxyacetone: Al molar ratio = 14:1, 90 °C, 10 mg dihydroxyacetone in 2 g water over 4–24 h. DHA, PA, and LA indicates dihydroxyacetone, pyruvaldehyde, and lactic acid, respectively.

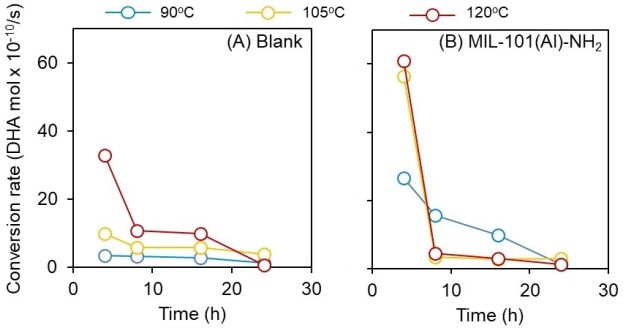

Figure 5. Effect of MIL-101(Al)–NH_2 catalysts and reaction temperature on dihydroxyacetone conversion rate. Reaction condition. dihydroxyacetone (DHA): Al molar ratio = 14:1 and 10 mg DHA in 2 g water.

valdehyde. To test this possibility, we used dihydroxyacetone as a reactant in water without catalysts. We heated the reaction to 90, 105, and 120 °C (Figure **S3**). Dihydroxyacetone conversion increased with increasing temperature. Pyruvaldehyde was the main reaction product. We did not observe lactic acid, which suggested that dihydroxyacetone isomerization required acid catalysts. Pyruvaldehyde yield increased and reached a maximum of 24% after 24 h at 105 °C. A further increase in reaction temperature to 120 °C decreased the pyruvaldehyde yield.

Next, we placed pyruvaldehyde in water without any catalyst and heated the solution at 90, 105, and 120 °C for 6 h (Figure S4). We found only a negligible amount of lactic acid produced (< 1%). This result suggested that Lewis acid sites were needed to convert pyruvaldehyde to lactic acid. Hossain et al. also reported the formation of pyruvaldehyde from heating a dilute solution of dihydroxyacetone at 140 °C,[46] in agreement with our findings. Although our results suggested that dihydroxyacetone dehydration was non-catalytic and reaction temperature mediated the dihydroxyacetone dehydration, we could not rule out a mediating activity of Lewis acid sites in MIL-101(Al)–NH_2.

Further, we compared the conversion rate of dihydroxyacetone dehydration with blank and MIL-101(Al)–NH_2 for 24 h (Figure 5). The dihydroxyacetone conversion rate decreased as a function of time because the dihydroxyacetone concentration became progressively depleted. The blank experiment (without catalyst) showed a low conversion rate of dihydroxyacetone at 90 and 105 °C (0.1–1.0 nmol/s). The dihydroxyacetone conversion rate increased to 3.4 nmol/s at 120 °C after 4 h. By adding MIL-101-Al–NH_2 as catalyst, the dihydroxyacetone conversion rate increased significantly to 6.1 nmol/s at 120 °C after 4 h. These results suggested that (1) reaction temperature facilitated the dihydroxyacetone dehydration at temperature > 105 °C, and (2) at lower temperature (90 °C), the Lewis acid sites in MIL-101(Al)–NH_2 were needed for the dihydroxyacetone dehydration step.

Effect of Lewis acid sites on pyruvaldehyde conversion and lactic acid stability

To decouple the activities of the MIL-101(Al)–NH_2 in pyruvaldehyde rehydration, we performed the same experiment with pyruvaldehyde as a reactant at 90 °C (Figure 6A). The Al-MOF increased lactic acid yield with time, and the yield reached 82% at 91% pyruvaldehyde conversion after 24 h. Interestingly, the lactic acid yield profiles with pyruvaldehyde as a reactant were similar to the yield with dihydroxyacetone as a reactant (Figure 3C). Next, we used lactic acid as a reactant with the Al-MOF catalyst (Figure 6B). We found that lactic acid was stable in Al-MOF at 90 °C with only 3.5% of conversion of lactic acid after 24 h. For γ-Al_2O_3, we ran the same experiment with pyruvaldehyde and lactic acid as reactants at 90 °C. We observed similar pyruvaldehyde conversion as Al-MOF but lower lactic acid yield (37% after 24 h) when using pyruvaldehyde as a reactant with γ-Al_2O_3 (Figure 6A). We observed a brown substance on the catalyst surface and reaction mixture due to the formation of humin, in agreement with previous studies.[46–47] With lactic acid

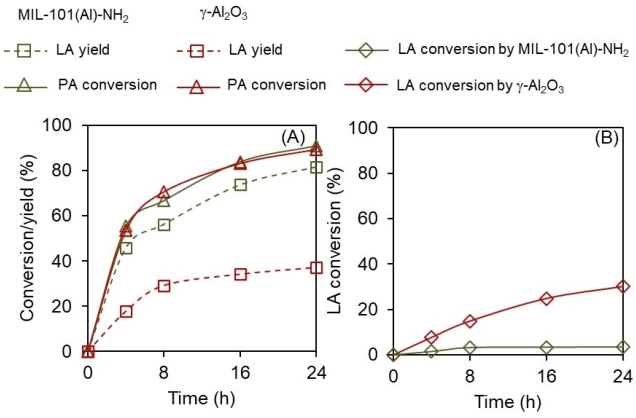

Figure 6. Catalytic activity of MIL-101(Al)–NH_2 and γ-Al_2O_3 using pyruvaldehyde (A) and lactic acid (B) as a feed. Reaction condition. pyruvaldehyde or lactic acid: Al molar ratio = 14:1, 90 °C, 8 mg pyruvaldehyde or 10 mg lactic acid in 2 g water. PA and LA indicates pyruvaldehyde and lactic acid, respectively.

alone, we observed a higher conversion of lactic acid (30%) with γ-Al_2O_3 than with Al-MOF (Figure 6B). These results suggested that Al-MOF did not catalyze side reactions or degradation of lactic acid. Together, these results suggested that Al-MOF was selective to lactic acid and stable in the presence of lactic acid.

Effect of reaction temperature on the dihydroxyacetone isomerization by MIL-101(Al)–NH_2

To determine the effect of reaction temperature on the catalytic performance of MIL-101(Al)–NH_2, we ran the dihydroxyacetone isomerization reaction in water using MIL-101(Al)–NH_2 at 90, 105, and 120 °C (Figure S5). As a control, we used γ-Al_2O_3 as the solid Lewis acid catalyst and ran the dihydroxyacetone isomerization reaction in water at 90, 105, and 120 °C as well (Fig S6). Pyruvaldehyde and lactic acid were major reaction products. The evolution of pyruvaldehyde yield had a volcano shape, which suggested that pyruvaldehyde was an intermediate. Using γ-Al_2O_3, we found that the dihydroxyacetone conversion and lactic acid yield increased with time and reaction temperature. For γ-Al_2O_3, dihydroxyacetone conversion and yield of pyruvaldehyde and lactic acid showed similar behaviors at 105 and 120 °C. We found a high dihydroxyacetone conversion of 95% and a 44% lactic acid yield at 120 °C after 24 h (Figure S6). These results suggested that 105 °C was the optimal reaction temperature for γ-Al_2O_3. For MIL-101(Al)–NH_2, increased reaction time and temperature progressively increased the dihydroxyacetone conversion and lactic acid yield. We obtained the highest yield of lactic acid (~89%) at 97% dihydroxyacetone conversion at 120 °C after 24 h (Figure S5). These results suggested that Lewis acid sites were required for the formation of lactic acid in water regardless of reaction temperature (90–120 °C), which corroborated our blank experiments (Figure S3).

Stability and reusability of MIL-101(Al)–NH_2 in dihydroxyacetone conversion

To evaluate the catalyst stability under the reaction condition, we performed the filtration experiments by conducting the DHA isomerization using Al-MOF over 8 h at 90 °C, filtering the Al-MOF catalyst from the reaction mixture, and heating the filtrate under the same reaction condition (90 °C) for 16 h (Figure 7A). We sampled the reaction mixture 3 times during 16 h and measured dihydroxyacetone conversion and lactic acid yield. The dihydroxyacetone conversion and pyruvaldehyde yield increased slightly during the prolonged 16 h, in line with our dihydroxyacetone conversion with blank (Figure S3A). Whereas the yield of lactic acid remained constant. These results suggested that (1) there was a minimal Al species leaching from Al-MOF into the reaction mixture, (2) lactic acid was stable at 90 °C over 16 h, (3) pyruvaldehyde rehydration to lactic acid required catalysts.

The ability to recycle catalysts is important for their practical use. We recycled the MIL-101(Al)–NH_2 by centrifugation and

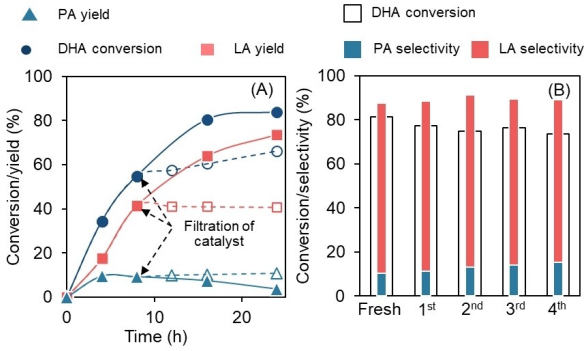

Figure 7. Stability and reusability of Al-MOFs for the dihydroxyacetone isomerization by filtration test at 90 °C (A) and recycle of MIL-101(Al)–NH_2 catalyst at 120 °C, 4 h (B). Reaction condition. dihydroxyacetone: Al molar ratio = 14:1. DHA, PA, and LA indicates dihydroxyacetone, pyruvaldehyde, and lactic acid, respectively.

washing with water to remove the residual products, intermediates, and unreacted dihydroxyacetone. The catalyst was then dried in a vacuum oven at 130 °C to remove moisture. We selected this temperature based on our TGA results to minimize the decomposition of Al-MOFs. The Al-MOF catalyst maintained the catalytic performance with a < 7% drop in dihydroxyacetone conversion and retained its lactic acid selectivity (73%) for four cycles (Figure 7B). We also observed the pyruvaldehyde selectivity increased slightly over time. This slight increase in pyruvaldehyde selectivity was hypothesized because of a slight loss of Lewis acid sites and blockage of active sites. Further, we characterized the spent Al-MOF catalyst after 4th reuse cycle by ICP-OES, XRD, FTIR, and DRIFTS (Figure S1 and S7). The aluminum content of the spent catalyst, measured by ICP-OES, was 11.0 wt.%, similar to that of the fresh catalysts (11.6 wt.%), which suggested minimal aluminum leaching even after 4 recycles. The XRD, FTIR, and DRIFT spectra of the spent catalyst exhibited similar chemical structure, functionality, and acid properties to those of fresh Al-MOF, which suggested minimal changes in chemical structure and acid properties of the Al-MOF after reuse. Together, these filtration and characterization results suggested catalyst stability under the present experimental conditions. Overall, MIL-101(Al)–NH_2 maintained high lactic acid selectivity for all the cycles and structural integrity after four recycles.

Discussion

We investigated the catalytic performance of MIL-101(Al)–NH_2 for dihydroxyacetone isomerization in water. The challenge in dihydroxyacetone isomerization to lactic acid is the development of active and selective solid acid catalysts. The dihydroxyacetone isomerization reaction is a cascade in which (1) dihydroxyacetone is dehydrated to pyruvaldehyde, followed by (2) pyruvaldehyde rehydrated to lactic acid. We found that the dihydroxyacetone dehydration to pyruvaldehyde is a non-catalytic reaction and can be accelerated in the presence of

Lewis acids, whereas pyruvaldehyde rehydration to lactic acid requires the Lewis acid sites (Figure S4). Moreover, we found that Al-MOFs are active and selective toward pyruvaldehyde rehydration to lactic acid.

The most significant finding was that Al-MOF was a water-tolerant solid Lewis acid catalyst that selectively catalyzed the conversion of dihydroxyacetone to lactic acid. In Table S4, we summarized the activity of selected catalysts for dihydroxyacetone isomerization into lactic acid. Homogeneous Al salts showed high selectivity to lactic acid (90%) (entry 16).[9] However, homogeneous catalysts need to be separated from the products, which complicates the conversion process. Zeolites have high catalytic activity for the dihydroxyacetone isomerization and high lactic acid yield (entries 2–8).[14,46,48] Sn-containing solid catalysts showed high lactic acid selectivity (> 90%) with complete dihydroxyacetone conversion (entries 3, 9).[49–50] However, the synthesis of Sn-containing solid catalysts is complex and requires long crystallization times.[51] Most solid Lewis acid catalysts react with water and decompose or deactivate over time.[52–53] For example, Lewis acidic H-USY-6 zeolite is effective for the isomerization of triose sugars to lactic acid. Still, coke formation and irreversible framework damage occur when lactic acid is produced under aqueous conditions.[48] Takagaki et al. used boehmite γ-AlO(OH) as a solid Lewis acid catalyst for the dihydroxyacetone isomerization in water and observed 32% lactic acid selectivity at complete dihydroxyacetone conversion. Christensen et al. used Sn-Beta for the isomerization of dihydroxyacetone in water. They observed severe catalyst deactivation due to the formation of large carbonaceous deposits, which decreased the formation of lactic acid.[54] MOFs have sponge-like crystal structures, which are ideal for water capture.[55–56] However, water could either displace the bound ligand, collapse the MOF structure, or block the active sites (metal nodes) and prevent the accessibility of reactants to the metal nodes.[57] In addition, MOFs are unstable in aqueous media.[58–60] Many MOFs, including Mg-MOFs,[61] MOF-5,[62–63] IRMOF-1,[64] deactivate rapidly in water. Our results demonstrated that MIL-101(Al)–NH_2 was water-tolerant and possessed Lewis acidity for selective dihydroxyacetone isomerization to lactic acid.

Another significant finding was that Lewis acid sites enhanced dihydroxyacetone dehydration to pyruvaldehyde. The activity of acid sites for dihydroxyacetone dehydration is controversial.[65–66] Liu et al.[67] and Kim et al.[68] used Sn-MFI and Sn-MCM-41 catalysts for the conversion of dihydroxyacetone. They found that both Brønsted and Lewis acid sites were important for the selective production of lactic acid. Brønsted acids catalyzed dihydroxyacetone dehydration to pyruvaldehyde, and Lewis acids catalyzed pyruvaldehyde rehydration to lactic acid. In contrast, Santos et al.[69] reported that the water-tolerant Lewis acid Nb_2O_5 had high catalytic activity (75% selectivity at 160 °C) to transform glyceraldehyde into lactic acid. However, they did not assess the reusability of Nb_2O_5. Surprisingly, our findings revealed that common solid Lewis acid catalysts, such as γ-Al_2O_3, were active but not selective to dihydroxyacetone isomerization to lactic acid. One possible reason is because lactic acid acted as a Brønsted acid catalyst and competed with the Lewis acidic sites of γ-Al_2O_3; this competition promoted side reactions and product degradation,[66] which corroborated our findings of the instability of lactic acid in the presence of γ-Al_2O_3. In this current work, we further extended our previous study[46] by demonstrating that, although the reaction temperature facilitated the dihydroxyacetone dehydration, the added solid Lewis acidic Al-MOF catalysts enhanced the dihydroxyacetone conversion and pyruvaldehyde selectivity.

When starting with dihydroxyacetone, we observed pyruvaldehyde and lactic acid as reaction products, in line with the cascade reaction pathway and pyruvaldehyde as an intermediate. On the basis of the foregoing findings, Figure 8 shows a proposed mechanism for dihydroxyacetone dehydration on MIL-101(Al)–NH_2 catalyst. The reaction proceeds by (1) keto-enol tautomerization of dihydroxyacetone to enediol derivative, (2) dehydration of enediol derivative to pyruvaldehyde, and (3) pyruvaldehyde rehydration on MIL-101(Al)–NH_2 to form lactic acid.

First, dihydroxyacetone interacts with Lewis acidic Al sites of MIL-101(Al)–NH_2 through its carbonyl and hydroxyl groups and then undergoes a keto-enol tautomerization to enediol derivative, compound **A**. The presence of Lewis acidic MIL-101(Al)–NH_2 accelerates the keto-enol tautomerization and subsequent dehydration by activating carbonyl and hydroxyl groups of dihydroxyacetone. Second, dehydration of enediol results in the enol form of pyruvaldehyde, which is subsequently tautomerized into pyruvaldehyde.[70–71] Third, the pyruvaldehyde undergoes rehydration into lactic acid by MIL-

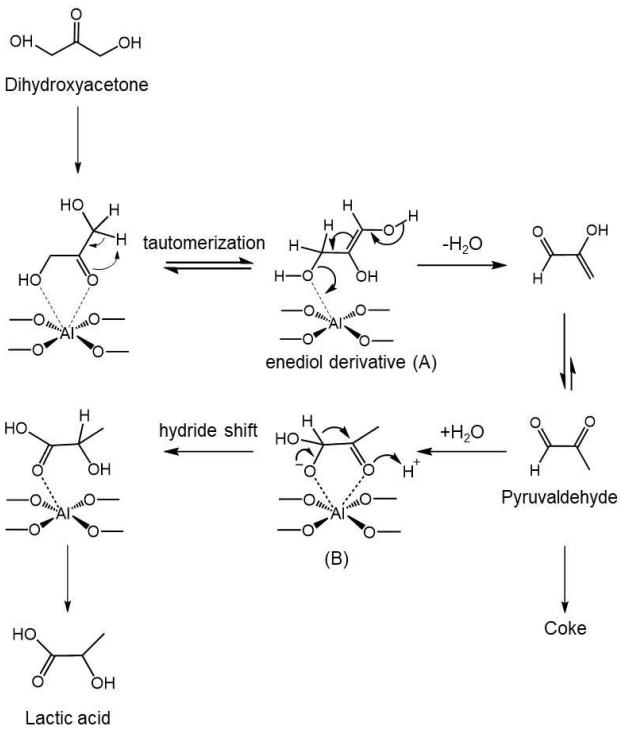

Figure 8. Proposed chemical pathway for the dihydroxyacetone conversion to lactic acid by MIL-101(Al)–NH_2.

101(Al)–NH_2. In this step, the Lewis acidic sites of MIL-101(Al)–NH_2 generate protons by dissociation of H_2O molecules and activate the carbon of the carbonyl group into a specific intermediate, compound **B**. Subsequently, a 1,2-hydride shift of compound **B** on Lewis acidic Al sites of MIL-101(Al)–NH_2 occurs by shifting proton from methine carbon to carbonyl carbon. Simultaneously abstraction of proton generated from H_2O dissociation by the carbonyl oxygen enables the formation of lactic acid product. The Lewis acidic MIL-101(Al)–NH_2 was responsible for the selective pyruvaldehyde rehydration to lactic acid.

Our findings provide a new understanding of the water-tolerant Lewis acidic MIL-101(Al)–NH_2 for selective dihydroxyacetone isomerization to lactic acid. The development of water-tolerant and recyclable solid Lewis acid catalysts remains a challenge in lactic acid production. The understanding gained from this work can guide the design of selective solid catalysts and control reaction temperature to maximize the lactic acid yield. Moreover, the use of water-tolerant Lewis acidic MIL-101(Al)–NH_2 could be extended to other aqueous acid-catalyzed biomass conversion reactions, such as isomerization,[72] Meerwein-Ponndorf-Verley reduction,[73] Fries rearrangement,[74] acetalization,[75] hydrolysis,[76] esterification,[77] condensation,[78] and dehydration.[79]

Conclusion

We present a new catalytic strategy for dihydroxyacetone isomerization to lactic acid by Lewis acidic MIL-101(Al)–NH_2 metal-organic framework (MOF). We found that the Lewis acidic MIL-101(Al)–NH_2 MOF facilitated the dehydration of dihydroxyacetone to pyruvaldehyde. The Lewis acidic MIL-101(Al)–NH_2 MOF enhanced the subsequent pyruvaldehyde rehydration to lactic acid. These findings underscore the importance of MIL-101(Al)–NH_2 as a promising water-tolerant Lewis acid catalyst for lactic acid production. Further research may extend this work by investigating the cooperative effect of temperature and Lewis acidic MIL-101(Al)–NH_2 MOF, elucidating the function of amino groups in the linker, and developing of the techno-economic analysis model for the feasibility of using Al-MOF as catalyst.

Experimental Section

Materials

All chemicals were used as received unless otherwise noted. Table S1 lists their CAS numbers, purity, and manufacturers.

Synthesis of metal-organic framework

The MIL-101(Al)–NH_2 metal-organic frameworks (MOFs) were synthesized with a slight modification of the solvothermal method.[30] Typically, a mixture of aluminum chloride hexahydrate (0.51 g, 2 mmol) and 2-aminoterephthalic acid (0.56 g, 3 mmol) in 30 mL dimethylformamide (DMF) was kept without stirring in a Teflon-lined autoclave reactor at 130 °C for 72 h. Then the reactor was cooled to ambient temperature, and the solids were separated from the solution by centrifugation (6000 RPM, 5 min). Next, the solids were washed with DMF under sonication for 10 min and followed by washing with methanol at ambient temperature. Then the solid catalysts were kept in hot (70 °C) methanol for 5 h and dried under vacuum at 80 °C for overnight.

Characterization of the catalysts

The metal content and physiochemical properties of the synthesized catalysts were determined by X-ray diffraction (XRD), N_2 adsorption-desorption, thermogravimetric analysis (TGA), high-resolution transmission electron microscopy (HRTEM), inductively coupled plasma-optical emission spectroscopy (ICP-OES), Fourier-transform infrared spectroscopy (FTIR), and diffuse reflectance infrared Fourier transform spectroscopy (DRIFTS).

X-ray diffraction

X-ray diffraction (XRD) analysis of samples was conducted on a Bruker AXS Model D8 Advance A28 diffractometer (Germany) using Cu$K\alpha$ radiation in the 2θ range from 5° to 40° with 0.02 degree/step. Samples of 200 mg were used in each analysis.

N_2 adsorption-desorption measurement

The surface area, pore size, and pore volume of the catalysts were calculated from N_2 adsorption-desorption measured by a Micromeritics Tristar (Norcross, GA, USA) instrument. The TriStar was calibrated with reference materials (Micromeritics, Norcross, GA, USA). Prior to the measurement, the sample was pretreated at 130 °C for 4 h using a Micromeritics FlowPrep with sample degasser (Norcross, GA, USA). The surface area, S_{BET}, was determined from N_2 isotherms by Brunauer-Emmett-Teller equation (BET) at −196.15 °C.[80–81] The BET surface area was calculated in the range of relative pressures between 0.05 and 0.3. The pore volume was estimated from the N_2 desorption values according to the Barrett-Joyner-Halenda (BJH) model.[82] The pore volume was calculated as the uptake (cm^3/g) at a relative pressure of 0.95. The average pore size of the samples was measured by the BJH model.[83–84]

Thermogravimetric analysis

To determine the thermal stability of catalysts, thermogravimetric analysis (TGA) was performed with an SDT Q600 TA instrument (New Castle, DE, USA). In short, ~20 mg of the sample was placed in a cylindrical alumina crucible and heated in the air from ambient temperature to 700 °C with a heating rate of 10 °C/min under N_2 flow (100 ml/min). The change in weight of samples was used to determine the moisture content, decomposition of the linkers, and formation of metal oxides.

Transmission electron microscopy and energy-dispersive X-ray spectroscopy analysis

To determine the microstructure and elemental distribution of the catalysts, high-resolution transmission electron microscopy (HRTEM) was performed using a Tecnai F20 (FEI company, OR, USA) microscope operating at 200 kV. The HRTEM specimens were prepared by dispersing small amounts of catalysts onto Cu grid-supported holey carbon films. For the analysis of the microstructure, scanning transmission electron microscopy (STEM) images were acquired using a high annular angle dark field (HAADF)

detector (E.A. Fischione Instruments, Inc., PA, USA) and an electron probe of a 1 nm diameter. In addition, energy-dispersive X-ray spectroscopy (EDS) maps for the elemental distribution analysis were collected using a TEAM EDS (EDAX, Inc., NJ, USA) spectrometer.

Inductively coupled plasma-optical emission spectroscopy

The metal content of the catalysts was determined by inductively coupled plasma-optical emission spectroscopy (ICP-OES). ICP-OES measurements were performed using a 100 mg sample dissolved in 10 mL of nitric acid. Heating was used to ensure that the sample was completely dissolved. Once cooled, the sample was further diluted to 25 mL with double distilled water. Measurements were acquired on a Varian 720-ES spectrometer equipped with a seaspray nebulizer and cyclonic class spray chamber. Parameters included a sample intake of 1 mL/min, argon plasma flow rate of 15 L/min, and an auxiliary gas (Ar) flow rate of 1.5 L/min. The instrument was calibrated using certified reference materials manufactured by VHG™ Instrument (LGC Standards USA, NH, USA).

Fourier transform infrared spectroscopy

Infrared spectra of samples were recorded on a JASCO Fourier transform infrared (FTIR) spectrometer (Easton, MD, USA), equipped with an attenuated total reflection stage (ATR). Samples of 5 mg were used in each analysis. The samples were scanned between 400 and 4000 cm^{-1} at a 4 cm^{-1} resolution. Spectra were collected using a deuterated triglycine sulfate (DTGS) detector averaging 256 scans.

Diffuse reflectance infrared Fourier transform spectroscopy

Diffuse reflectance infrared Fourier transform spectroscopy (DRIFTS) with adsorbed pyridine was performed to characterize the acid sites. The temperature-programmed desorption was conducted with the JASCO FTIR equipped with a high-temperature DiffuseIR™ cell (PIKE Technology, WI, USA). The sample treatment and DRIFTS experiments with temperature-programmed desorption were conducted with a slight modification as described.[85] In short, the MOF sample (~5 mg) was placed in a cylindrical alumina crucible and treated in N_2 gas (50 mL/min) at 130 °C for 60 min unless otherwise noted. After the pretreatment, the sample was cooled to 30 °C. The DRIFT spectrum of fresh catalyst was recorded as the background spectrum. The samples were then saturated with pyridine vapor by the flow of N_2 gas (50 mL/min). Then the physisorbed pyridine was removed by flushing with N_2 gas (50 mL/min) at 50, 100, or 150 °C for 30 min before recording the DRIFT spectra. All spectra were recorded with 256 scans between 4000–400 cm^{-1} at a 4 cm^{-1} resolution. The amount of Lewis acid sites at each desorption temperature was calculated from the integrated area of bands (after background subtraction) of adsorbed pyridine at 1067 cm^{-1} and 1445 cm^{-1}[86] Because of the limited thermal stability of Al-MOF, a lower desorption temperature (maximum 150 °C) was used.

Isomerization of dihydroxyacetone

Approximately 10 mg dihydroxyacetone and 2 g water were added to a 25 mL pressure tube in an oil bath. The catalyst was loaded using a dihydroxyacetone:Al molar ratio of 14:1, unless otherwise noted. The pressure tube was sealed and stirred at 600 rpm (to minimize mass transfer limitations), unless otherwise noted. The reaction was stopped by quenching in a cold-water bath, then water (~5 mL) was added to dissolve the remaining dihydroxyacetone and products. The solution was centrifuged, and the residual solids were removed. The liquid sample was analyzed for products and unreacted reactants.

Product analysis and quantification

The reactants and products were analyzed by High-Performance Liquid Chromatography (HPLC, Agilent Technology, Santa Clara, CA, USA) equipped with a refractive index detector (RID) and diode array detector(DAD). An Aminex HPX-87H (300×7.8 mm, Bio-Rad®, Hercules, CA, USA) was used for reactants and product separation at 60 °C with 0.6 mL/min 4 mM H_2SO_4 as a mobile phase. The concentration of reactants and products was determined by the peak area from the RID signals. Reactants and reaction products were calibrated against certified standards (Absolute Standards, Inc., Hamden, CT, USA). The dihydroxyacetone conversion, product yield, and product selectivity were calculated using Equations (1)–(6):

$$\text{Dihydroxyacetone conversion } (\%) = \frac{\text{dihydroxyacetone reacted (mol)}}{\text{initial dihydroxyacetone (mol)}} \times 100 \quad (1)$$

$$\text{Product yield } (\%) = \frac{\text{product generated (mol)}}{\text{initial dihydroxyacetone (mol)}} \times 100 \quad (2)$$

$$\text{Product selectivity } (\%) = \frac{\text{product yield}}{\text{dihydroxyacetone conversion}} \times 100 \quad (3)$$

$$\text{TOF } (h^{-1}) = \frac{\text{dihydroxyacetone reacted (mol)}}{\text{metal (mol)} \times \text{time (h)}} \quad (4)$$

$$\text{TON} = \frac{\text{dihydroxyacetone reacted (mol)}}{\text{metal (mole)}} \quad (5)$$

$$\text{Productivity } (h^{-1}) = \frac{\text{Lactic acid formed (mole)}}{\text{metal (mole)} \times \text{time (h)}} \times 100 \quad (6)$$

Acknowledgements

A part of this material is based upon work supported by the National Science Foundation under Cooperative Agreement No. 1355438 and Internal Research Grant, Office of the Executive Vice President for Research, University of Louisville. This work was performed in part at the Conn Center for Renewable Energy Research at the University of Louisville, which belongs to the National Science Foundation NNCI KY Manufacturing and Nano Integration Node, supported by ECCS-1542174. The authors would like to thank Dr. Howard Fried for his valuable comments and suggestions on the manuscript.

Conflict of Interest

The authors declare no conflict of interest.

Data Availability Statement

The data that support the findings of this study are available from the corresponding author upon reasonable request.

Keywords: dihydroxyacetone · isomerization · metal-organic frameworks · lactic acid · Lewis acids

[1] M. Dusselier, P. Van Wouwe, A. Dewaele, E. Makshina, B. F. Sels, *Energy Environ. Sci.* **2013**, *6*, 1415–1442.
[2] P. Ponchai, K. Adpakpang, S. Thongratkaew, K. Chaipojjana, S. Wannapaiboon, S. Siwaipram, K. Faungnawakij, S. Bureekaew, *Chem. Commun.* **2020**, *56*, 8019–8022.
[3] S. Kiatphuengporn, A. Junkaew, C. Luadthong, S. Thongratkaew, C. Yimsukanan, S. Songtawee, T. Butburee, P. Khemthong, S. Namuangruk, M. Kunaseth, *Green Chem.* **2020**, *22*, 8572–8583.
[4] L. Yang, J. Su, S. Carl, J. G. Lynam, X. Yang, H. Lin, *Appl. Catal. B* **2015**, *162*, 149–157.
[5] Y. Zhang, H. Luo, L. Kong, X. Zhao, G. Miao, L. Zhu, S. Li, Y. Sun, *Green Chem.* **2020**, *22*, 7333–7336.
[6] C. Kosri, S. Kiatphuengporn, T. Butburee, S. Youngjun, S. Thongratkaew, K. Faungnawakij, C. Yimsukanan, N. Chanlek, P. Kidkhunthod, J. Wittayakun, *Catal. Today* **2021**, *367*, 205–212.
[7] M. Morales, P. Y. Dapsens, I. Giovinazzo, J. Witte, C. Mondelli, S. Papadokonstantakis, K. Hungerbühler, J. Pérez-Ramírez, *Energy Environ. Sci.* **2015**, *8*, 558–567.
[8] P. Y. Dapsens, B. T. Kusema, C. Mondelli, J. Pérez-Ramírez, *J. Mol. Catal. A* **2014**, *388*, 141–147.
[9] C. B. Rasrendra, B. A. Fachri, I. G. B. N. Makertihartha, S. Adisasmito, H. J. Heeres, *ChemSusChem* **2011**, *4*, 768–777.
[10] M. Xia, W. Dong, M. Gu, C. Chang, Z. Shen, Y. Zhang, *RSC Adv.* **2018**, *8*, 8965–8975.
[11] E. Jolimaitre, D. Delcroix, N. Essayem, C. Pinel, M. Besson, *Catal. Sci. Technol.* **2018**, *8*, 1349–1356.
[12] Y. Sun, L. Shi, H. Wang, G. Miao, L. Kong, S. Li, Y. Sun, *Sustain. Energy Fuels* **2019**, *3*, 1163–1171.
[13] L. Kong, Z. Shen, W. Zhang, M. Xia, M. Gu, X. Zhou, Y. Zhang, *ACS Omega* **2018**, *3*, 17430–17438.
[14] P. Y. Dapsens, C. Mondelli, J. Pérez-Ramírez, *ChemSusChem* **2013**, *6*, 831–839.
[15] M. K. Wardani, G. T. Kadja, A. T. Fajar, I. Makertihartha, M. L. Gunawan, V. Suendo, R. R. Mukti, *RSC Adv.* **2019**, *9*, 77–86.
[16] M. Gackowski, K. Tarach, J. Podobiński, S. Jarczewski, P. Kuśtrowski, J. Datka, *Microporous Mesoporous Mater.* **2018**, *263*, 282–288.
[17] D. Farrusseng, S. Aguado, C. Pinel, *Angew. Chem. Int. Ed.* **2009**, *48*, 7502–7513; *Angew. Chem.* **2009**, *121*, 7638–7649.
[18] J. Lee, O. K. Farha, J. Roberts, K. A. Scheidt, S. T. Nguyen, J. T. Hupp, *Chem. Soc. Rev.* **2009**, *38*, 1450–1459.
[19] G. Férey, *Chem. Soc. Rev.* **2008**, *37*, 191–214.
[20] S. Horike, D. Umeyama, S. Kitagawa, *Acc. Chem. Res.* **2013**, *46*, 2376–2384.
[21] H. B. Wu, X. W. D. Lou, *Sci. Adv.* **2017**, *3*, eaap9252.
[22] K. Sumida, D. L. Rogow, J. A. Mason, T. M. McDonald, E. D. Bloch, Z. R. Herm, T. Bae, J. R. Long, *Chem. Rev.* **2012**, *112*, 724–781.
[23] I. A. Lazaro, R. S. Forgan, *Coord. Chem. Rev.* **2019**, *380*, 230–259.
[24] H. Furukawa, F. Gandara, Y. Zhang, J. Jiang, W. L. Queen, M. R. Hudson, O. M. Yaghi, *J. Am. Chem. Soc.* **2014**, *136*, 4369–4381.
[25] J. Canivet, A. Fateeva, Y. Guo, B. Coasne, D. Farrusseng, *Chem. Soc. Rev.* **2014**, *43*, 5594–5617.
[26] N. C. Burtch, H. Jasuja, K. S. Walton, *Chem. Rev.* **2014**, *114*, 10575–10612.
[27] M. Ding, X. Cai, H. Jiang, *Chem. Sci.* **2019**, *10*, 10209–10230.
[28] M. Ding, H. Jiang, *CCS* **2021**, *3*, 2740–2748.
[29] S. Yuan, L. Feng, K. Wang, J. Pang, M. Bosch, C. Lollar, Y. Sun, J. Qin, X. Yang, P. Zhang, *Adv. Mater.* **2018**, *30*, 1704303.
[30] L. Bromberg, X. Su, T. A. Hatton, *ACS Appl. Mater. Interfaces* **2013**, *5*, 5468–5477.
[31] T. Toyao, M. Fujiwaki, Y. Horiuchi, M. Matsuoka, *RSC Adv.* **2013**, *3*, 21582–21587.
[32] E. V. Ramos-Fernandez, C. Pieters, B. van der Linden, J. Juan-Alcañiz, P. Serra-Crespo, M. Verhoeven, H. Niemantsverdriet, J. Gascon, F. Kapteijn, *J. Catal.* **2012**, *289*, 42–52.
[33] P. Serra-Crespo, E. V. Ramos-Fernandez, J. Gascon, F. Kapteijn, *Chem. Mater.* **2011**, *23*, 2565–2572.
[34] V. I. Isaeva, A. L. Tarasov, L. E. Starannikova, Y. P. Yampol'skii, A. Y. Alent'ev, L. M. Kustov, *Russ. Chem. Bull.* **2015**, *64*, 2791–2795.
[35] B. Seoane, C. Téllez, J. Coronas, C. Staudt, *Sep. Purif. Technol.* **2013**, *111*, 72–81.
[36] J. E. Samad, J. Blanchard, C. Sayag, C. Louis, J. R. Regalbuto, *J. Catal.* **2016**, *342*, 213–225.
[37] J. Jiang, O. Yaghi, *Chem. Rev.* **2015**, *115*, 6966–6997.
[38] J. N. Hall, P. Bollini, *ACS Catal.* **2020**, *10*, 3750–3763.
[39] X. X. Zheng, Z. P. Fang, Z. J. Dai, J. M. Cai, L. J. Shen, Y. F. Zhang, C. T. Au, L. L. Jiang, *Inorg. Chem.* **2020**, *59*, 4483–4492.
[40] C. Volkringer, H. Leclerc, J. C. Lavalley, T. Loiseau, G. Ferey, M. Daturi, A. Vimont, *J. Phys. Chem. C* **2012**, *116*, 5710–5719.
[41] H. Leclerc, A. Vimont, J.-C. Lavalley, M. Daturi, A. Wiersum, P. Llwellyn, P. Horcajada, G. Férey, C. Serre, *Phys. Chem. Chem. Phys.* **2011**, *13*, 11748–11756.
[42] C. Volkringer, H. Leclerc, J.-C. Lavalley, T. Loiseau, G. Ferey, M. Daturi, A. Vimont, *J. Phys. Chem. C* **2012**, *116*, 5710–5719.
[43] S. Yamaguchi, M. Yabushita, M. Kim, J. Hirayama, K. Motokura, A. Fukuoka, K. Nakajima, *ACS Sustainable Chem. Eng.* **2018**, *6*, 8113–8117.
[44] G. R. Jenness, M. A. Christiansen, S. Caratzoulas, D. G. Vlachos, R. J. Gorte, *J. Phys. Chem. C* **2014**, *118*, 12899–12907.
[45] T. K. Phung, C. Herrera, M. Á. Larrubia, M. García-Diéguez, E. Finocchio, L. J. Alemany, G. Busca, *Appl. Catal. A* **2014**, *483*, 41–51.
[46] M. A. Hossain, K. N. Mills, A. M. Molley, M. S. Rahaman, S. Tulaphol, S. B. Lalvani, J. Dong, M. K. Sunkara, N. Sathitsuksanoh, *Appl. Catal. A* **2021**, *611*, 117979.
[47] A. Takagaki, J. C. Jung, S. Hayashi, *RSC Adv.* **2014**, *4*, 43785–43791.
[48] R. M. West, M. S. Holm, S. Saravanamurugan, J. Xiong, Z. Beversdorf, E. Taarning, C. H. Christensen, *J. Catal.* **2010**, *269*, 122–130.
[49] A. Feliczak-Guzik, M. Sprynskyy, I. Nowak, B. Buszewski, *Catalysts* **2018**, *8*, 31.
[50] X. Wang, F. Liang, C. Huang, Y. Li, B. Chen, *Catal. Sci. Technol.* **2016**, *6*, 6551–6560.
[51] M. Moliner, Y. Román-Leshkov, M. E. Davis, *PNAS* **2010**, *107*, 6164–6168.
[52] S. Kobayashi, in *Organic synthesis in water*, Springer, **1998**, pp. 262–305.
[53] T. Ollevier, *Bismuth-mediated organic reactions, Vol. 311*, Springer Science & Business Media, **2012**.
[54] E. Taarning, S. Saravanamurugan, M. S. Holm, J. Xiong, R. M. West, C. H. Christensen, *Conversion of Oxygenates over Zeolite Catalysts: Structure-Activity Relations* **2009**, 90.
[55] M. W. Logan, S. Langevin, Z. Xia, *Sci. Rep.* **2020**, *10*, 1–11.
[56] N. Hanikel, M. S. Prévot, F. Fathieh, E. A. Kapustin, H. Lyu, H. Wang, N. J. Diercks, T. G. Glover, O. M. Yaghi, *ACS Cent. Sci.* **2019**, *5*, 1699–1706.
[57] K. Tan, N. Nijem, Y. Gao, S. Zuluaga, J. Li, T. Thonhauser, Y. J. Chabal, *CrystEngComm* **2015**, *17*, 247–260.
[58] N. ul Qadir, S. A. M. Said, H. M. Bahaidarah, *Microporous Mesoporous Mater.* **2015**, *201*, 61–90.
[59] T. Wu, L. Shen, M. Luebbers, C. Hu, Q. Chen, Z. Ni, R. I. Masel, *Chem. Commun.* **2010**, *46*, 6120–6122.
[60] M. Bosch, M. Zhang, H. Zhou, *Adv. Chem.* **2014**, *2014*, 1155.
[61] E. Mangano, J. Kahr, P. A. Wright, S. Brandani, *Faraday Discuss.* **2016**, *192*, 181–195.
[62] Y. Ming, N. Kumar, D. J. Siegel, *ACS Omega* **2017**, *2*, 4921–4928.
[63] H. Li, W. Shi, K. Zhao, H. Li, Y. Bing, P. Cheng, *Inorg. Chem.* **2012**, *51*, 9200–9207.
[64] J. G. Nguyen, S. M. Cohen, *J. Am. Chem. Soc.* **2010**, *132*, 4560–4561.
[65] Y. Sun, L. Shi, H. Wang, G. Miao, L. Kong, S. Li, Y. Sun, *Sustain. Energy Fuels* **2019**, *3*, 1163–1171.
[66] W. Dong, Z. Shen, B. Peng, M. Gu, X. Zhou, B. Xiang, Y. Zhang, *Sci. Rep.* **2016**, *6*, 1–8.
[67] Y. Liu, Y. Xiao, C. Xia, X. Yi, Y. Zhao, J. Yuan, K. Huang, B. Zhu, A. Zheng, M. Lin, *J. Catal.* **2020**, *391*, 386–396.
[68] K. Kim, Z. Wang, Y. Jiang, M. Hunger, J. Huang, *Green Chem.* **2019**, *21*, 3383–3393.
[69] K. Santos, E. Albuquerque, G. Innocenti, L. Borges, C. Sievers, M. Fraga, *ChemCatChem* **2019**, *11*, 3054–3063.
[70] C. Rasrendra, B. Fachri, I. Makertihartha, S. Adisasmito, H. Heeres, *ChemSusChem* **2011**, *4*, 768–777.
[71] Y. Hayashi, Y. Sasaki, *Chem. Commun.* **2005**, *21*, 2716–2718.
[72] S. Saravanamurugan, M. Paniagua, J. A. Melero, A. Riisager, *JACS* **2013**, *135*, 5246–5249.
[73] A. H. Valekar, M. Lee, J. W. Yoon, J. Kwak, D. Hong, K. Oh, G. Cha, Y. Kwon, J. Jung, J. Chang, *ACS Catal.* **2020**, *10*, 3720–3732.

[74] M. S. Rahaman, S. Tulaphol, A. M. Molley, K. N. Mills, M. A. Hossain, D. Yelle, T. Maihom, N. Sathitsuksanoh, *Dalton Trans.* **2021**, *50*, 17390–17396.
[75] M. S. Rahaman, T. K. Phung, M. A. Hossain, E. Chowdhury, S. Tulaphol, S. B. Lalvani, M. O'Toole, G. A. Willing, J. B. Jasinski, M. Crocker, *Appl. Catal. A* **2020**, *592*, 117369.
[76] S. Tulaphol, M. A. Hossain, M. S. Rahaman, L. Liu, T. K. Phung, S. Renneckar, N. Grisdanurak, N. Sathitsuksanoh, *Energy Fuels* **2019**, *34*, 1764–1772.
[77] Y. Xu, Z. Wang, H. Tan, K. Jing, Z. Xu, G. Guo, *Catal. Sci. Technol.* **2020**, *10*, 1699–1707.
[78] M. S. Rahaman, S. Tulaphol, M. A. Hossain, C. N. Evrard, L. M. Thompson, N. Sathitsuksanoh, *J. Mol. Catal.* **2021**, *514*, 111848.
[79] M. S. Rahaman, S. Tulaphol, M. A. Hossain, J. B. Jasinski, N. Sun, A. George, B. A. Simmons, T. Maihom, M. Crocker, N. Sathitsuksanoh, *Fuel* **2022**, 310, 122459.
[80] R. Haul, Wiley Online Library, **1982**.
[81] K. S. W. Sing, *Pure Appl. Chem.* **1985**, *57*, 603–619.
[82] E. P. Barrett, L. G. Joyner, P. P. Halenda, *J. Am. Chem. Soc.* **1951**, *73*, 373–380.
[83] J. Xu, J. Liu, Z. Li, X. Wang, Z. Wang, *J. Mater. Sci.* **2019**, *54*, 12911–12924.
[84] S. K. Jana, R. Nishida, K. Shindo, T. Kugita, S. Namba, *Microporous Mesoporous Mater.* **2004**, *68*, 133–142.
[85] A. I. Osman, J. K. Abu-Dahrieh, D. W. Rooney, S. A. Halawy, M. A. Mohamed, A. Abdelkader, *Appl. Catal. B* **2012**, *127*, 307–315.
[86] D. Yu, M. Wu, Q. Hu, L. Wang, C. Lv, L. Zhang, *J. Hazard. Mater.* **2019**, *367*, 456–464.

Manuscript received: November 18, 2021
Revised manuscript received: December 12, 2021
Accepted manuscript online: December 13, 2021
Version of record online: ■■, ■■■

RESEARCH ARTICLE

Lactic acid by water-tolerant solid Lewis acidic Al-MOF! This study finds the dihydroxyacetone dehydration to pyruvaldehyde is non-catalytic. The Lewis acids of Al-MOF improve catalytic activity of dihydroxyacetone dehydration to pyruvaldehyde and catalyze rehydration of the resulting pyruvaldehyde to lactic acid in water. This catalyst is stable and reusable.

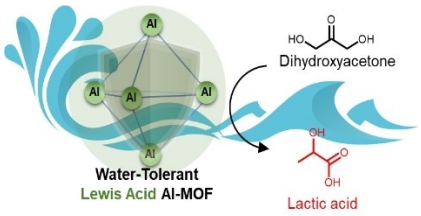

M. S. Rahaman, Dr. S. Tulaphol, K. Mills, A. Molley, M. A. Hossain, Prof. S. Lalvani, Dr. T. Maihom, Prof. M. Crocker, Prof. N. Sathitsuksanoh**

1 – 11

Aluminum-based Metal-Organic Framework as Water-tolerant Lewis Acid Catalyst for Selective Dihydroxyacetone Isomerization to Lactic Acid